Effect of Diluents on the Crystallization Behavior of Poly(4-Methyl-1-Pentene) and Membrane Morphology via Thermally Induced Phase Separation

Haijun Tao,[1] Jun Zhang,[1] Xiaolin Wang[2]

[1]*College of Materials Science and Engineering, Nanjing University of Technology, Nanjing, 210009, China*
[2]*Department of Chemical Engineering, Tsinghua University, Beijing 100084, China*

Received 24 October 2006; accepted 26 November 2007
DOI 10.1002/app.27808
Published online 23 January 2008 in Wiley InterScience (www.interscience.wiley.com).

ABSTRACT: The effect of diluents on polymer crystallization and membrane morphology via thermally induced phase separation(TIPS) were studied by changing the composition of the mixed-diluents systematically, in the system of poly(4-methyl-1-pentene) (TPX)/dibutyl-phthalate (DBP)/di-*n*-octyl-phthalate (D-*n*-OP) with TPX concentration of 30 wt %. The TPX crystallization was observed with differential scanning calorimetry (DSC) and wide angle X-ray diffraction (WAXD). The membranes were characterized with scanning electron microscopy (SEM), porosity, and pore size measurement. As the content of D-*n*-OP increased in mixed-diluents, the solubility with TPX increased, inducing the phase separation changing from liquid–liquid phase separation into solid–liquid phase separation, which changed the membrane morphology and structure. When the ratios of DBP to D-*n*-OP were 10 : 0, 7 : 3; 5 : 5, and 3 : 7, membranes were formed with cellular structure and well connected pores, while the ratio was 0 : 10, discernable spherulities were found with not well-formed pore structure. The effect of composition of the mixed-diluents on membrane morphology was more remarkable in TPX/dioctyl-sebacate (DOS)/dimethyl-phthalate (DMP) system, since good cellular structure was formed when the ratios of DOS to DMP were 10 : 0, 7 : 3, while spherulites were observed when 5 : 5. Dual endotherm peaks behavior on DSC melting curves emerged for all the samples in this study, which was attributed to the special polymer crystallization behavior, primary crystallization, and secondary crystallization occurred when quenching the samples. As the content of D-*n*-OP increased, the secondary crystallization enhanced which induced the first endotherm peak on DSC melting curves moving to a lower temperature and the broadening of the overall melting peak, as well as the increasing of the overall crystallinity. J Appl Polym Sci 108: 1348–1355, 2008

Key words: membrane; thermally induced phase separation; diluent; poly(4-methyl-1-pentene); crystallization

INTRODUCTION

During the thermally induced phase separation process, a homogeneous solution needs to be formed by the dissolution of a polymer in a diluent at a high temperature, and then phase separation is induced by cooling the solution. Thus, the selection of the diluent is very important, since the compatibility of polymer and diluent affects not only the thermodynamic properties, such as the binodal line and crystallization temperature in phase diagram, but also the kinetics of droplet growth. The compatibility of polymer and diluent is one of the key factors affecting the membrane morphology, which could be studied in terms of the solubility parameter, $\delta((J/cm^3)^{1/2})$.

In a typical liquid–liquid (L–L) phase separation diagram, the binodal line locates above the crystallization temperature, forming a L–L phase separation region. As the solubility becomes stronger, the binodal line shifts to a lower temperature, as shown by the arrow in Figure 1,[1,2] while the crystallization temperature is less influenced. In other words, the L–L phase separation region decreases as the difference of the solubility parameter between the polymer and diluent($\Delta\delta_{p\text{-}d}$) becomes smaller. The L–L phase separation shifts below the crystallization temperature as the interaction between the components increases with the use of good solvent,[1,2] and solid–liquid (S–L) phase separation will occur. So the phase separation could be changed from L–L phase separation in a poor solvent system into S–L phase separation with a good solvent, although keeping the thermal quench depth constant, since the relative driving force for L–L and S–L phase separation can be varied by the diluents.

The interaction of polymer and diluent will be different with the changing of the end-groups, or the molecule of the diluent and the ratio of the two diluents in a ternary system. So when these factors change, the phase separation mechanisms and the membrane morphology will be different.

Isotactic polypropylene (iPP)[3] membrane was formed via TIPS with methyl salicylate (MS), diphenyl

Correspondence to: J. Zhang (zhangjun@njut.edu.cn)

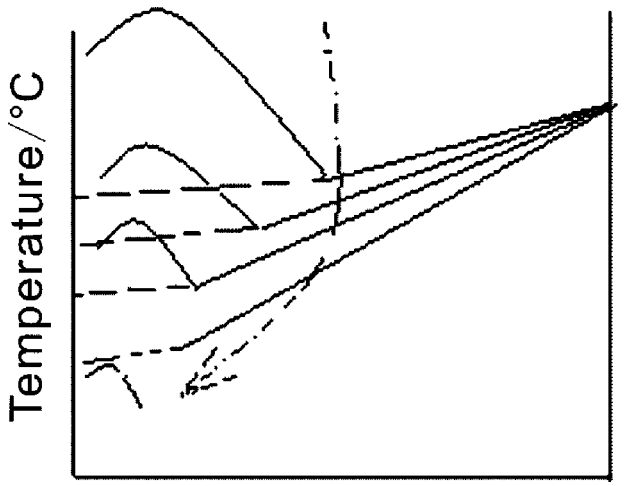

Figure 1 The composite phase separation diagram of L–L and S–L phase separation. Dashed line: the crystallization temperature; solid curve: binodal line.

ether (DPE), and diphenyl methane (DPM) as di luents, respectively. The solubility parameters of iPP and these three diluents were 18.8, 21.7, 20.7, 19.5 $((J/cm^3)^{1/2})$, respectively. So in the order of MS, DPE, DPM, the cloud point curve shifted to a lower temperature, since the solubility of diluent was in the order of MS, DPE, DPM. However, the crystallization temperature was not influenced much by the diluent type. The diluents with different end-groups[2] structure will result in different interactions with the polymer and then the phase diagrams. Eicosane ($C_{20}H_{42}$), eicosanoic acid ($C_{19}H_{39}COOH$), and n,*n*-bis(2-hydroxyethyl) tallowamine (TA) were chosen to investigate the relationship between membrane structure and thermodynamic interaction. The iPP/$C_{20}H_{42}$ sample showed a spherulitic structure resulting from S–L phase separation only. In iPP/$C_{19}H_{39}COOH$ system, no discernible spherulites were found because the phase separation occurred prior to iPP crystallization, which restricted subsequent iPP crystallization. In iPP/TA system typical L–L phase separation occurred prior to iPP crystallization, which would form cellular membrane structure. A series of diluents[4] of poly(ethylene glycol) (PEG) with different molecular weight were used in nylon12/diluent systems via TIPS. As the molecular weight of PEG increased from 200 to 600, the phase boundary shifted to a higher temperature, and the monotectic composition of nylon12 increased, while the crystallization line inside the liquid–liquid phase envelope was almost horizontal. When molecular weight of PEG was higher than 1000, nylon12 did not form miscible blends with PEG below the thermal degradation temperature, since the solubility of PEG to nylon12 decreased as the increase of the molecular weight. A series of dialkyl phthalates[5] with different number of carbon atoms in the alkyl chain were used as the diluents in iPP/diluents systems. As the number of carbon atoms increased, the interaction became favorable and the L–L phase separation temperature decreased, whereas the melting temperature was constant. In the iPP/C_6 (6 means the number of carbon atoms) system, the L–L phase separation located above the melting temperature when the concentration was between 3 and 10 wt %, but below the melting temperature when the concentration was 10–40 wt %. With a better solvent, C_7, the L–L phase separation shifted below the melting points on the whole concentration region including the highest temperature at which the liquid–liquid phase separation was observed. This highest temperature decreased further when a better solvent, C_8, was used.

A ternary mixture of polymer/diluent/diluent could be considered as a pseudobinary system[6,7] during TIPS process. The phase diagrams can be controlled successfully by varying the composition of the two diluents, then the interaction, systematically. For example, in high density polyethylene (HDPE)/ditrydecylphthalate/hexadecane system, the L–L phase separation temperature decreased significantly with a favorable interaction to polymer (by increasing the composition of hexadecane in the solvent mixture) while the melting point curve remained constant. In EVOH/1,3-propanediol/glycerol system[8] the solubility parameter of them were 21.4, 24.0, 33.8 $((J/cm^3)^{1/2})$, respectively. As the ratio of 1,3-propanediol to glycerol increased, the solubility of the diluents increased, and the cloud point shifted to lower temperature. In the 1,3-propanediol to glycerol ratio 0 : 100 system, L–L phase separation happened and only cellular pores were formed. Changing the mixed-diluents ratio into 20 : 80, the spherulitic structure due to both polymer crystallization and cellular pores was obtained, attributing to the sequential occurrence of L–L phase separation just after polymer crystallization. However, only the spherulities were observed in both the 50 : 50 and 100 : 0 systems, because the polymer crystallization occurred before L–L phase separation.

The kinetics of droplet growth also differed from each other when the diluents were different. When the iPP/diluents systems were quenched and the temperature was maintained at a constant value,[3] the droplet growth rate decreased in the order of iPP/MS, iPP/DPE, iPP/DPM, since the matrix phase viscosity decreased in the order of MS, DPE, DPM. When the solution was cooled at a constant cooling rate, the difference in the droplet sizes in three systems was pronounced, attributed to the difference in the time interval in the phase diagrams for the droplet growth. When the molecular weight of PEG in nylon12/PEG systems changed,[4] the equilibrium domain size increased, which could be attributed to the increase in interfacial tension as a function of molecular weight. In EVOH/1,3-propanediol/glycerol system,[8] a faster growth rate and large structure were obtained in the

1,3-propanediol to glycerol ratio 0 : 100 pure glycerol system due to a higher T_{cloud}. However, in the 50 : 50 and 100 : 0 diluent systems, the structure hardly grew in experimental time-scale.

TPX membranes were prepared by various methods,[9–12] however, in this article the TPX membrane was prepared via TIPS and the effect of diluents on membrane structure and morphology was investigated by changing the ratio of DBP to D-*n*-OP in the TPX/DBP/D-*n*-OP system and the ratio of DOS to DMP in TPX/DOS/DMP system. The phase separation would be different with various mixed-diluents, which would then affect the membrane structure and morphology. Meanwhile the crystallization of TPX during TIPS process may also be influenced by different diluents. It was speculated that lots of isobutyls in the TPX main chain would restrict the mobility of the polymer chain and then affect the crystallization of TPX just like the effect of ethyls to hydrogenated polybutadiene.[13] The crystallization behavior of TPX in the systems with different mixed-diluents was concerned with the help of DSC and WAXD analysis.

EXPERIMENTS

Materials

Membranes were prepared with the systems of TPX/DBP/D-*n*-OP and TPX/DOS/DMP. The polymer, TPX (MX-002) was purchased from Mitsui, Japan. DBP(AR) and DMP(AR) purchased from Qidong Shenyao Chemical Reagents, China, while D-*n*-OP(CP) Shanghai Lingfeng Chemical Reagents, China, and DOS(CP) Shandong Haihua Tianhe Organic chemical, China. Methanol(AR) and i-butanol(AR) were supplied by Shanghai Lingfeng Chemical Reagents, China, and used without further purification.

Membrane preparation

Appropriate amounts of polymer (30 wt %) and diluents were measured into a test tube, which was then placed into an oil bath kept at 250°C ± 2°C with low stirring for 4 h. Then the mixture was cooled at ambient temperature for 30 min, yielding a solid polymer/diluents sample. The solid sample was chopped into small pieces, which were placed in a tailor-made test tube, a ram-type copper tube with the inner and outer diameters of 10 and 12 mm, respectively, sealed by the copper plunger. After reheating in an oven for 15 min at 250°C, the test tube was taken out to quench at the experimental temperature (90°C in this study) for a certain time (15 min) followed by quenching to 0°C immediately. Finally the diluents were extracted from the membrane with methanol. The extractants were evaporated in a vacuum oven (ZK-82A, Shanghai Laboratory Apparatus Company, China) and the membrane was gained.

Characterization of the membrane

Scanning electron microscopy

SEM micrographs were taken by a Kash SX-40 (Japan) scanning electron microscope. Each of the samples was fractured under liquid nitrogen, and coated with gold using a sputtering coater, and the cross section was scanned. The pore sizes of a certain number of pores on the SEM micrographs were measured with the Sigmascan software.

Porosity

The ultimate TPX membranes were immersed in i-butanol for 24 h, and weighed immediately after removing the i-butanol from the surface. The porosity (A_k) was calculated according to the formula:

$$A_k = \frac{(W_2 - W_1)\rho_1}{\rho_1 W_2 + (\rho_2 - \rho_1)W_1} \times 100\ \%$$

where W_1 is the initial membrane weight; W_2 is the immersed membrane weight; ρ_1 is the density of TPX, taken as 0.83 g/cm^3[3,14] and ρ_2 is the density of i-butanol, taken as 0.8 g/cm^3.

Characterization of the polymer crystallization

Differential scanning calorimetry analysis

TPX crystallization in the TPX/DBP/D-*n*-OP system was followed through differential scanning calorimetry (DSC) measurement on Perkin–Elmer DSC-7C (America), and the endotherm peaks were recorded to fully characterize the thermal behavior. Measurements were made on 6 mg solid polymer/diluents sample. The sample was first heated to 250°C at 10°C/min and kept at this temperature for 2 min. Then the sample was cooled to 50°C at 5°C/min. In this case, on the DSC curve, the temperature where the exotherm shows the peak is denoted as peak crystallization temperature, T_p. The temperature where the exotherm initially departs from the baseline is taken as the onset temperature, T_{onset}. The degree of crystallinity (X_c) was calculated according to the formula:

$$X_c = \frac{\Delta H_f / C}{\Delta H_f^*} \times 100\%$$

where ΔH_f is the endothermic heat during the melting process and ΔH_f^* is the heat of fusion of a perfect crystal, taken as 117.2 J/g[14] for TPX. The C is the concentration of TPX in the polymer/diluents systems.

Wide angle X-ray diffraction

For wide angle X-ray diffraction (WAXD) measurement, additional samples of about 1×1 cm^2 with the average thickness of about 0.1 mm were made at the same condition in which the membranes were made. Small pieces of the solid polymer/diluents sample were melted onto a microscope slides at 250°C, and quenched at 90°C for 15 min, then quenched immediately to 0°C. The XRD-6000 (Shimadzw, Japan) was used in this study, the current was 30 mA, the accelerating voltage was 40 kV, and the scanning rate 4°/min over the 2θ range from 60° to 5° using Cu Kα radial. For further analysis, the interplanar spacing d and the thickness of the lamellar crystal D values were calculated according to the Bragg and Scherrer equations respectively, as following[15,16]:

$$d = \lambda/(2\sin(\theta))$$

$$D = k\lambda/(\beta\cos(\theta))$$

where the λ is the wavelength of the X-ray, taken as 0.1542 nm, θ is the half scanning angle, k is Scherrer constant, taken as 0.89, and β is the full width at half maximum (FWHM) of the diffraction peak (measured in radian).

RESULTS AND DISCUSSION

Effect of the diluents composition on membrane structure

A series of TPX/diluents samples of different diluents composition were prepared, by changing the weight ratio of DBP to D-*n*-OP systematically. TPX/diluents samples of polymer concentration of 30 wt % were made as described above, and the reheated tailor-made test tube with small sample pieces in it was quenched at 90°C for 15 min. As shown in Table I, the solubility of the mixed-diluents to TPX increases as the weight ratio of DBP to D-*n*-OP decreases. The compositive solubility parameter δ_c was estimated according to the equation[16] $\delta_c = \delta_1\varphi_1 + \delta_2\varphi_2$, where δ_1 and δ_2 were the solubility parameters of the two diluents, φ_1 and φ_2 were the volume fraction, respectively. The detailed data were listed in Table I. As the content of D-*n*-OP in the mixed-diluents increased, it changed from a weak solvent into a better solvent, and the phase separation may change from L–L phase separation to S–L phase separation although the exact phase separation diagram was not determined here. Five samples with the weight ratio of DBP to D-*n*-OP of 10 : 0, 7 : 3, 5 : 5, 3 : 7, and 0 : 10 were prepared and made into membranes. Figure 2 is the SEM photographs of these five samples.

TABLE I
The Data of TPX Membranes with the Composite Diluents of Different Ratio of DBP to D-*n*-OP

Weight ratio of DBP to D-*n*-OP	10/0	7/3	5/5	3/7	0/10
Solubility parameter δ_c ($(J/cm^3)^{1/2}$)	19[14]	18.12	17.55	17.0	16.2[14]
Average diameter (μm)	2.05	1.01	0.89	0.71	0.48
Porosity A_k (%)	17.7	40.0	62.4	67.6	64.2

Cellular morphology of the membranes are visible in Figure 2(a–d), which are the result of L–L phase separation[17] characteristically, occurring in the systems with poor solvent. In Figure 2(e), discernible spherulites and some pores are observed, attributed to the occurring of S–L phase separation accompanying with the L–L phase separation with a better solvent.[8,18] In a poor solvent system, L–L phase separation happens and the single-phase solution at higher temperature separates into polymer-rich phase and diluent-rich phase. Complete and well-connected pores, or so-called cellular morphology, are formed during this process. As the solubility becomes stronger, the binodal line shifts to a lower temperature and the region for L–L phase separation reduces. So when quenched at a constant temperature of 90°C in this study for the first four samples, the coarsening time decreased when the content of DBP decreased and the pore size decreased too because of the decreasing of droplet growth. When the ratio of DBP to D-*n*-OP changed from 10 : 0 to 7 : 3, 5 : 5, and 3 : 7, the average pore sizes decreased remarkably, which are 2.05, 1.01, 0.89, and 0.71 μm, respectively, with 65.4% decreasing. With a further decreasing of the content of DBP, the mixed-diluents became a better solvent for TPX, and the binodal line went below the crystallization temperature, causing the change from L–L phase separation into S–L phase separation as shown in Figure 1. In Figure 2(e), spherulitic structure formed from S–L phase separation via nucleation and growth of the polymer with accompanying rejection of the liquid diluent to interspherulitic and intraspherulitic regions.[18] The pore structure was damaged, and only a part of the pore sizes were complete which could be estimated with the Sigmascan software. As shown in Table I the porosity increased from 17.71 to 67.57% as the pore size decreased from 2.05 to 0.71 μm, since the pore density in every area increased and the wall of the pores decreased. The detailed data are listed in Table I.

The effect of the ratio of one diluent to another in the mixed-diluents on the membrane via TIPS was more remarkable in the TPX/DOS/DMP system. When the ratio of DOS to DMP was settled at 10 : 0, 7 : 3, and 5 : 5, the polymer/diluents samples could be mixed. However, when the ratio changed into 3 : 7 or 0 : 10, no homogeneous solution could be attained below the thermal degradation temperature, since the

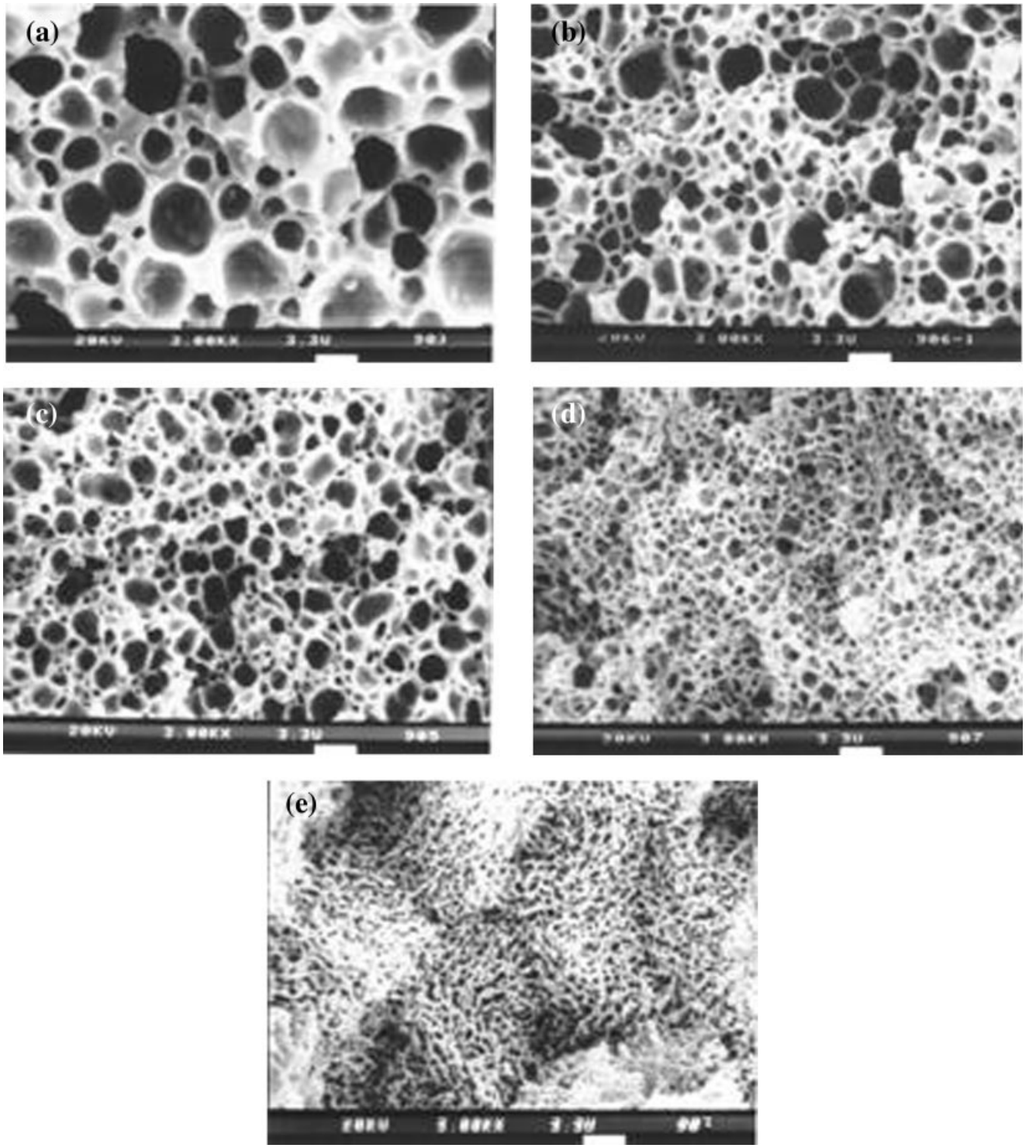

Figure 2 SEM photographs of the cross section of TPX membranes with different ratio of DBP to D-*n*-OP. (×3 K). a, 10 : 0; b, 7 : 3; c, 5 : 5; d, 3 : 7; e, 0 : 10.

solubility decreased so much while the solubility parameters of the mixed-diluents were 20.39, 21.9 $(J/cm^3)^{1/2}$ with great difference from the 16.8 $(J/cm^3)^{1/2}$ of TPX. From the SEM photographs in Figure 3(a,b), good cellular structure were formed resulting from L–L phase separation, and lamellar crystal and spherulites were observed in Figure 3(c) which formed during the S–L phase separation.[2] So by changing the ratio in mixed-diluents systematically, the membrane morphology could be controlled according to different phase separation, L–L phase separation, S–L phase separation, or a competitive result of L–L and S–L phase separation. The data of these membranes made from TPX/DOS/DMP systems were listed in Table II in detail.[19]

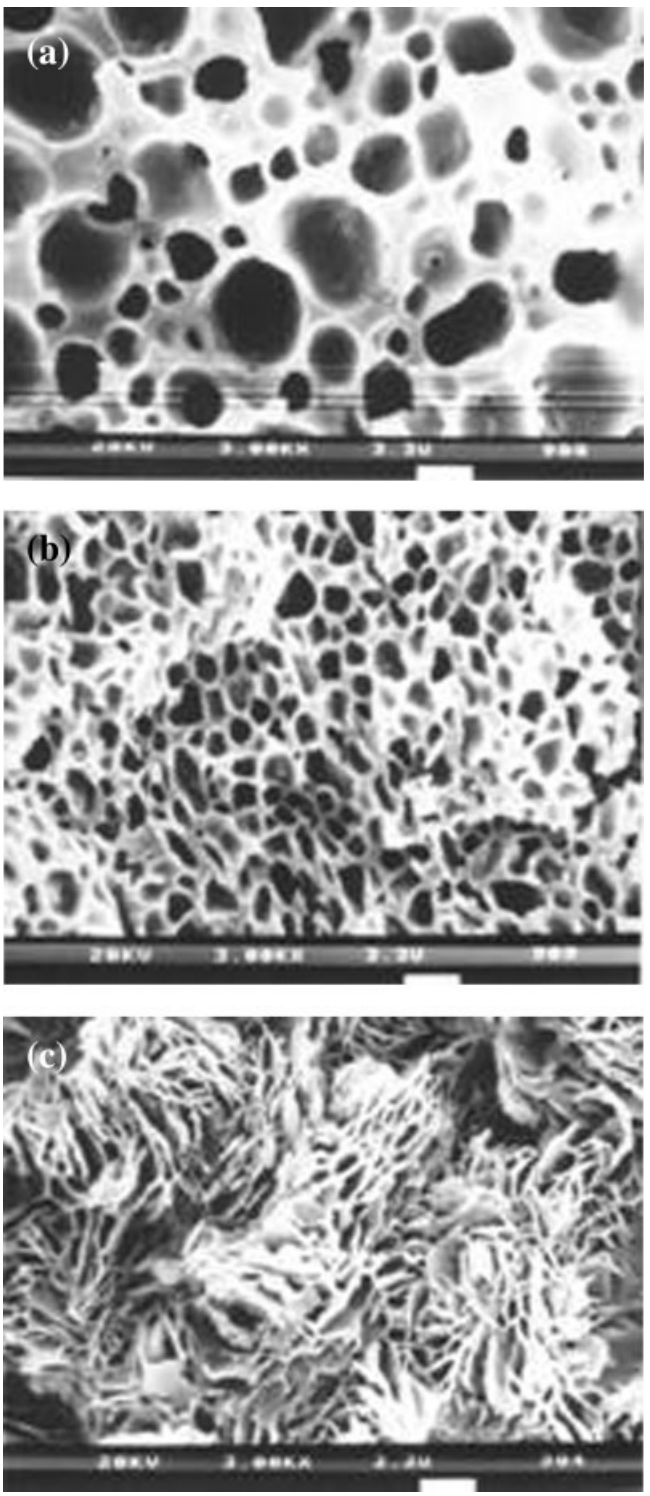

Figure 3 SEM photographs of the cross section of TPX membranes with different ratio of DOS to DMP. (×3 K). a, 5 : 5; b, 7 : 3; c, 10 : 0.

Effect of the diluents composition on polymer crystallization

In the TIPS process, the surpercooling temperature is a driving force for phase separation as well as the crystallization of polymer. In previous studies[12] TPX membranes were made via TIPS with DOS/DMP as diluents, and the crystallization behavior of TPX with different polymer concentrations and different quenching temperatures were observed. As the content of diluents increased, the crystallinity of TPX increased since the polymer chain could enter the crystal lattice with more diluents surrounding. In all the cases with different concentrations and quenching temperatures, dual endotherm peaks behavior on the melting traces of DSC was discovered. And with the quenching temperature increase, the first peak moved to a higher temperature while the second remained constant. This dual endotherm peaks behavior was attributed to the TPX crystals of different crystallization extent formed in TIPS process because of the special chain structure with a lot of isobutyls in the main chain. In this study the crystallization behavior of TPX in mixed-diluents with different diluents composition was observed with DSC and WAXD analysis.

TABLE II
The Data of TPX Membranes with the Composite Diluents of Different Ratio of DOS to DMP

Weight ratio of DOS to DMP	0/10	3/7	5/5	7/3	10/0
Solubility parameter δ_c ($(J/cm^3)^{1/2}$)	21.9[14]	20.39	19.46	18.66	17.6[14]
Porosity A_k (%)	*[a]	*[a]	24.78	41.82	63.26
Average diameter (μm)			2.53	1.40	*[b]

[a] No homogenous solution was mixed.
[b] No well structured pores were attained.

Figure 4 is the melting traces of DSC of the five samples. As shown, there are two endotherms of every melting trace. According to the detailed results listed in Table III, the second peak occurred at about 203°C

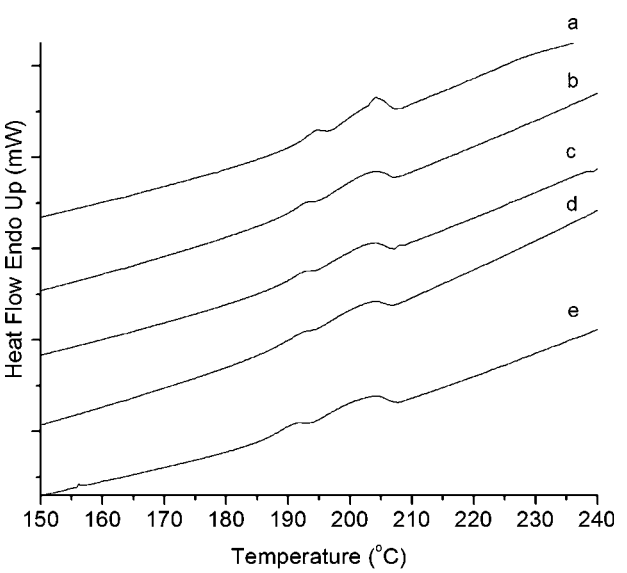

Figure 4 The melting traces of TPX/DBP/D-*n*-OP systems with different weight ratio of DBP to D-*n*-OP. a, 10 : 0; b, 7 : 3; c, 5 : 5; d, 3 : 7; e, 0 : 10.

TABLE III
The Detailed DSC Results of the Samples with Different Ratio of DBP to D-*n*-OP

Weight ratio of DBP to D-*n*-OP	δ_c $(J/cm^3)^{1/2}$	T_m (°C)					ΔH (J g^{-1})	X_c%
		T_{peak1}	T_{peak2}	T_{onset}	T_{end}	ΔT		
10 : 0	19.0	195.0	204.1	191.3	207.2	15.9	2.48	7.05
7 : 3	18.12	193.2	202.4	189.2	207.3	18.1	3.39	9.65
5 : 5	17.55	192.7	202.0	188.4	206.5	18.3	3.42	9.74
3 : 7	17.0	192.8	202.1	188.5	206.6	18.1	3.48	9.91
0 : 10	16.2	191.9	202.0	185.7	207.8	22.1	4.17	11.87

$\Delta T = T_{end} - T_{onset.}$

for all the five samples, while the first one moved to a lower temperature in the order of a, b, c, d and e. Moreover, in the order of a, b, c, d, and e, the T_{onset} of the first peak decreased, resulting in the widening of the whole endotherm peak. In previous studies of polypropylene (PP)[20] membranes via TIPS in the systems of PP/soybean oil/DBP, dual endotherm peaks behavior was observed and was attributed to the different crystal forms α-, β-PP with different melting temperatures. The WAXD results of the five systems above were in Figure 5 and Table IV. As shown the diffractograms of the systems with different mixed-diluents were almost the same, with intensity peaks emerging at 2θ of about 9.4°, 13.4°, 16.7°, 18.3°, and 20.6°, which are corresponding to the crystallographic planes (200), (220), (212), (321), and (113/411) of the same crystal form, form I.[21,22] It can be concluded that the ratio of DBP to D-*n*-OP had no effect on the crystal form of TPX in this study. Combining the studies in previous,[12] it was speculated that two crystallization, primary crystallization and secondary crystallization happened during the TIPS process because of the interrupting of the lot of isobutyls. The isocrystallization of semicrystalline polymers in some cases can be divided into two main steps.[23–25] The primary crystallization occurs in an unrestrained amorphous environment with no interferences on confinement of the crystals, resulting in the stable crystals with large extent of crystallization or large crystal particles. The secondary crystallization occurs in the amorphous chains or chain segments that are restricted or interfered by the crystals formed before, forming metastable crystals. Usually the primary crystals are thicker because they are formed in unrestricted spaces and secondary crystals are thinner since they are formed in a constrained space. So the whole of primary and secondary crystallization consists of thick parent lamellar crystals and thin crystals or said subsidiary branches in the interlamellar spaces.[24–26] Primary crystals thus melt at higher temperature during DSC process with a linear heating rate, and the thinner at lower temperature. If the thickness difference between primary and secondary crystals is significant, then

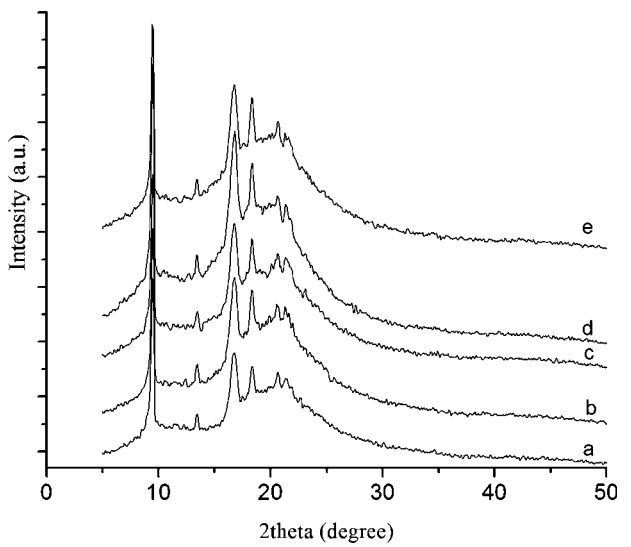

Figure 5 The WAXD of TPX/DBP/D-*n*-OP system with different weight ratio of DBP to D-*n*-OP. a, 10 : 0; b, 7 : 3; c, 5 : 5; d, 3 : 7; e, 0 : 10.

TABLE IV
Detailed Results of WAXD Analysis

		Samples				
	Peak	a	b	c	d	e
1	2θ (deg)	9.45	9.46	9.45	9.46	9.46
	I/I_{max} [a]	100	100	100	100	100
	d (Å)	9.36	9.35	9.35	9.35	9.36
	D (nm)	27.82	29.82	26.25	28.80	31.09
2	2θ (deg)	13.42	13.41	13.41	13.41	13.42
	I/I_{max}	10	12	9	10	9
	d (Å)	6.60	6.60	6.60	6.60	6.61
	D (nm)	35.11	28.13	33.88	37.26	34.88
3	2θ (deg)	16.70	16.75	16.75	16.69	16.69
	I/I_{max}	38	46	44	49	49
	d (Å)	5.31	5.29	5.31	5.31	5.29
	D (nm)	11.57	13.19	11.13	11.17	13.53
4	2θ (deg)	18.34	18.32	18.32	18.34	18.35
	I/I_{max}	25	31	31	32	35
	d (Å)	4.84	4.84	4.84	4.84	4.84
	D (nm)	16.30	18.95	16.83	15.52	18.67
5	2θ (deg)	20.60	20.55	20.60	20.60	20.60
	I/I_{max}	20	21	19	20	24
	d (Å)	4.31	4.32	4.31	4.31	4.31
	D (nm)	9.99	11.82	–	9.81	12.59

[a] Comparative intensity to the strongest peak.
d: the interplanar spacing.
D: the thickness of the lamellar crystal.

two melting endotherms are parted and observed on DSC melting curves during heating. Based on this hypothesis, the results in this study can be explained as following.

Although with different mixed-diluents, the primary crystals formed almost at the same temperature because of the unrestricted spaces, without much difference from each other, so with the same T_{p2} on the DSC melting curves. The secondary crystallization occurred in the interlamellar spaces with much interfering. What was more in this study, as the content of D-*n*-OP increased, the solubility of the mixed-diluents increased and the polymer chains could stretch easier resulting in a higher viscosity of the solution, which made the chain entering into the crystal lattice with great difficulties. The secondary crystallization in the high viscosity condition was much more defective and more crystals with smaller size or said lower extent formed, resulting in a wider statistic distribution of the size or crystallization extent of the crystals. In the study of isocrystallization of PET,[26] it was found that, as the molecular weight of PET increased, the mobility of the polymer chain reduced because of the more entanglements. More chain section of the polymer was rejected into the interlamellar spaces when the primary crystallization occurred. Then the proportion of the secondary crystals increased, and the first endotherm peak on the DSC melting curve enhanced. In this study, as the content of D-*n*-OP increased, the effect of the secondary crystallization increased because of the increasing viscosity. The crystallization process changed as the mixed-diluents differed, but the overall crystallinity increased from 7.05, 9.65, 9.74, 9.91 to 11.87% in the order of a, b, c, d and e.

A further analysis of the WAXD showed that there was no distinct regulation of the intensity, *d* and *D* values between the different samples. Medellin-Rodriguez[26] confirmed that the secondary crystalline structure would not give rise to the diffraction, just giving place to perceptive X-ray scattering but rather negligible X-ray diffraction. It may be concluded that the diluents with different composition had no effect on the primary crystallization but the secondary crystallization. This consisted with the results of the DSC analysis. So the difference of the secondary crystallization resulting from the different mixed-diluents affected the DSC melting curves and the overall crystallinity, but not the diffractograms.

CONCLUSIONS

The polymer crystallization and TPX membrane morphology were affected remarkably by the mixed-diluents via TIPS in this study. As the composition of the diluents changed, it could be changed from L–L phase separation in a poor solvent into S-L phase separation with a better solvent, and then the membrane morphology and properties differed. Cellular structure was formed when the ratio of DBP to D-*n*-OP was 10 : 0, 7 : 3, 5 : 5, 3 : 7 in the system of TPX/DBP/D-*n*-OP, and the pore size decreased in this order. But when the ratio was 0 : 10, discernable spherulitic structure was found because of the occurring of S–L phase separation accompanying with L–L phase separation. The effect of the composition of diluents was much more outstanding in the TPX/DOS/DMP systems. Primary crystallization and secondary crystallization occurred when quenching at 90°C for all the samples with different mixed-diluents in TPX/DBP/D-*n*-OP system. As the content of D-*n*-OP increased, the solubility increased and more crystals of smaller size formed during secondary crystallization, inducing the T_{onset} moving to a lower temperature and widening of the overall melting peak as well as the increasing of the crystallinity. However, the composition of the diluents or said solubility of the diluents had no distinct effect on the primary crystallization in this study.

References

1. Douglas, R. L.; Sung, S. K.; Kevin, E. K. J Membr Sci 1991, 64, 1.
2. Sung, S. K.; Douglas, R. L. J Membr Sci 1991, 64, 13.
3. Hideto, M.; Masaaki, T.; Shunsuke, K.; Yoshiro, K. J Appl Polym Sci 2001, 82, 169.
4. Cha, B. J.; Char, K.; Kim, J. J.; Kim, S. S.; Kim, C. K. J Membr Sci 1995, 108, 219.
5. Hwan, K. L.; Allan, S. M.; Kalle, L. Macromolecular 1992, 25, 4002.
6. Zhensheng, Y.; Heying, C.; Pingli, L.; Shichang, W. J Chem Ind Eng (China) 2005, 56, 981.
7. Hitesh, C. V.; Hwan, K. L.; Allan, S. M.; Kalle, L. J Membr Sci 1994, 89, 37.
8. Mengxian, S.; Hideto, M.; Masaaki, T.; Junpei, O.; Douglas, R. L. J Appl Polym Sci 2005, 95, 219.
9. Mohr, J. M.; Paul, D. R. Polymer 1991, 32, 1236.
10. Le Roux, J. D.; Paul, D. R. J Membr Sci 1992, 74, 233.
11. Lai, J.-Y.; Lin, F.-C. US Patent 5,628,942, 1997.
12. Tao, H.; Zhang, J.; Wang, X.; Gao, J. J Polym Sci Part B: Polym Phys 2007, 45, 153.
13. Zryd, J. L.; Burghardt, W. R. J Appl Polym Sci 1995, 57, 1525.
14. Cornelia, V.; Raymond, B. S., Eds. Handbook of Polyolefins-Synthesis and Properties; Marcel Dekker: New York, 1993.
15. Zhou, G., Ed. Polymer X-ray Diffraction; University of Science and Technology of China Press: He Fei, China, 1989.
16. Jin, R.; Hua, Y., Eds. Polymer Physicis, 2nd ed.; Chemical Industry Press: Beijing, China, 2000.
17. Graham, P. D.; McHugh, A. J. Macromolecules 1998, 31, 2565.
18. Kim, S. S.; Lim, G. B. A.; Alwattari, A. A.; Feng, W. Y.; Douglas, R. L. J Membr Sci 1991, 64, 41.
19. Dong, Y. Polymer Analysis Handbook; China Petrochemical Press: Beijing, China, 2004.
20. Luo, B.; Zhang, J.; Wang, X.; Wen, J. Acta Polym Sin 2007, 7, 866.
21. Charlet, G.; Delmas, G. Polymer 1984, 25, 1613.
22. Charlet, G.; Delmas, G. Polymer 1984, 25, 1619.
23. Carlos, A.; Avila-Orta; Medellin-Rodriguez, F. J.; Wang, Z.-G.; Damaso, N.-R.; Hsiao, B. S.; Yeh, F. Polymer 2003, 44, 1527.
24. Pakula, T. Polymer 1982, 23, 1300.
25. Bassett, D. C.; Olley, R. H.; Ai Rahei, I. A. M. Polymer 1988, 29, 1745.
26. Medellin-Rodriguez, F. J.; Phillips, P. J.; Lin, J. S.; Campos, R. J Polym Sci Part B: Polym Phys 1998, 36, 763.